Developmental Biology 331 (2009) 176–188

Contents lists available at ScienceDirect

Developmental Biology

journal homepage: www.elsevier.com/developmentalbiology

Requirement for *Twist1* in frontonasal and skull vault development in the mouse embryo

Heidi Bildsoe [a,b,1], David A.F. Loebel [a,b,*,1], Vanessa J. Jones [a], You-Tzung Chen [c], Richard R. Behringer [c], Patrick P.L. Tam [a,b]

[a] Embryology Unit, Children's Medical Research Institute, The University of Sydney, Locked Bag 23, Wentworthville, NSW 2145, Australia
[b] Sydney Medical School, The University of Sydney, Locked Bag 23, Wentworthville, NSW 2145, Australia
[c] Department of Molecular Genetics, University of Texas, M. D. Anderson Cancer Center, 1515 Holcombe Blvd, Houston, TX 77030, USA

ARTICLE INFO

Article history:
Received for publication 26 May 2008
Revised 27 April 2009
Accepted 27 April 2009
Available online 3 May 2009

Keywords:
Twist1
Cre
loxP
Neural crest cells
Craniofacial morphogenesis
Skeletal development

ABSTRACT

Using a Cre-mediated conditional deletion approach, we have dissected the function of *Twist1* in the morphogenesis of the craniofacial skeleton. Loss of *Twist1* in neural crest cells and their derivatives impairs skeletogenic differentiation and leads to the loss of bones of the snout, upper face and skull vault. While no anatomically recognizable maxilla is formed, a malformed mandible is present. Since *Twist1* is expressed in the tissues of the maxillary eminence and the mandibular arch, this finding suggests that the requirement for *Twist1* is not the same in all neural crest derivatives. The effect of the loss of *Twist1* function is not restricted to neural crest-derived bones, since the predominantly mesoderm-derived parietal and interparietal bones are also affected, presumably as a consequence of lost interactions with neural crest-derived tissues. In contrast, the formation of other mesodermal skeletal derivatives such as the occipital bones and most of the chondrocranium are not affected by the loss of *Twist1* in the neural crest cells.

Introduction

The skeleton of the skull, face and jaws develops from precursor tissues derived from two embryonic sources: the cranial neural crest (CNC) and the cranial paraxial mesoderm. In birds and mammals, the viscerocranium (skeleton of the jaw and face) is formed predominantly by skeletogenic cells derived from the CNC (Kuratani et al., 1997; Noden and Trainor, 2005; Abe et al., 2007) while the neurocranium (the vault and the base of the skull), contains both CNC and mesoderm derivatives. In the chick, the boundary between CNC- and mesoderm-derived bones in the skull vault lies within the frontal bones (Evans and Noden, 2006), whereas in mice this boundary lies in the coronal suture between the CNC-derived frontal bones and the mesoderm-derived parietal bones (Jiang et al., 2002; Yoshida et al., 2008). Underlying the cranial vault is the dura mater which, in the mouse, is composed of CNC-derived cells (Yoshida et al., 2008). Interactions with this tissue are required for the formation of the sutures and the ossification of the mesoderm-derived elements of the skull vault (Jiang et al., 2002;Gagan et al., 2007).

In mouse embryos, *Twist1*, which encodes a basic helix–loop–helix (bHLH) transcription factor, is expressed in the paraxial mesoderm surrounding the neural tube of the early-somite embryo (Fuchtbauer, 1995). Later, *Twist1* is expressed in the CNC-derived mesenchyme of the frontonasal region and in the branchial arches, which contain both CNC- and mesoderm-derived cells. *Twist1* is down-regulated in the branchial arch mesoderm by E9.5 (Fuchtbauer, 1995; Gitelman, 1997; Rinon et al., 2007). Loss of *Twist1* leads to major malformations of the craniofacial structures, suggesting that *Twist1* is required for the differentiation of CNC and mesoderm-derived tissues. *Twist1*-null mutant embryos also display closure defects of the cephalic neural tube (Chen and Behringer, 1995), despite the absence of *Twist1* expression in the neural tube. In chimaeras with a low (<25%) contribution of *Twist1*-null embryonic stem cells in the cranial mesenchyme, the brain and neural tube develop normally even when *Twist1*-deficient cells are present in the neuroepithelium (Chen and Behringer, 1995). This finding suggests that *Twist1* function is required specifically in the cranial mesenchyme for normal brain morphogenesis.

Absence of *Twist1* function impacts on the development of the CNC and the formation of CNC-derived tissues. *Twist1*-deficient CNC cells transplanted to the upper hindbrain of wild-type host embryos can initiate migration and home in to the first branchial arch. However, they fail to colonize the sub-ectodermal zone of the arch that is normally populated by the CNC cells. Instead, they are sequestered in the core of the arch where mesodermal cells are normally localized (Soo et al., 2002). *Twist1*-deficient cells are similarly localized to the

* Corresponding author. Embryology Unit, Children's Medical Research Institute, The University of Sydney, Locked Bag 23, Wentworthville, NSW 2145, Australia. Fax: +61 2 96872120.
E-mail address: dloebel@cmri.usyd.edu.au (D.A.F. Loebel).
[1] These authors contributed equally to the study.

0012-1606/$ – see front matter © 2009 Elsevier Inc. All rights reserved.
doi:10.1016/j.ydbio.2009.04.034

core of the branchial arch in chimeras generated from mutant ES cells and wild-type host embryos (Chen and Behringer, 1995).

Differentiation of branchial arch-derived tissues is compromised by the loss of *Twist1* function. *Sox10* activity is not down-regulated and *Aristaless*-related genes (*Cart1*, *Alx3* and *Alx4*) have not been activated in the mutant embryo at E10.5–11.5. However, explants of the first branchial arch from null mutant embryos can develop into teratomas containing CNC derivatives (skeletal and dental tissues) and mesoderm derivatives (muscles) (Soo et al., 2002). *Twist1*-null branchial arch tissues can therefore potentially form mandibular structures. However, the early demise of mutant embryos at mid-gestation has precluded further investigation of the full impact of the loss of *Twist1* function on the morphogenesis of the branchial arches and other craniofacial structures.

In the present study, we used Cre-mediated tissue-specific gene ablation to investigate the impact of loss of *Twist1* in CNC cells on craniofacial development using a conditional mutant strain with *Twist1* flanked by loxP sites (Chen et al., 2007). Ablation of *Twist1* in the CNC was achieved by expressing Cre recombinase under the control of regulatory elements of *Wnt1, Human plasminogen activator* (*HtPA*) and *Tyrosinase* genes. Our results reveal that *Twist1* activity is necessary to maintain CNC cells after migration and enable the formation of the cranial vault and the frontonasal, facial and jaw skeleton.

Materials and methods

Mouse strains

Twist1$^{3loxPneo/3loxPneo}$ mice, in which loxP sites flank the two exons of the *Twist1* gene (Chen et al., 2007), were maintained as a homozygous line and were phenotypically normal. These mice were mated with mice expressing an X-linked CMV-Cre transgene (Su et al., 2002) and the line maintained by selecting breeders from subsequent generations that were heterozygous for the deleted (del = null) allele, but did not carry the CMV-Cre transgene.

As a first step towards generating neural crest-specific *Twist1* deletions, *Twist1*$^{del/+}$ mice were crossed to each of three Cre-expressing lines: Wnt1-Cre (Danielian et al., 1998); HtPA-Cre (Pietri et al., 2003) and Tyr-Cre (Tonks et al., 2003). To reveal the activity of the Cre transgene, Cre transgenic mice were crossed to mice harboring a Z/AP reporter (Lobe et al., 1999).

Twist1$^{del/+}$; Wnt1-Cre, *Twist1*$^{del/+}$ HtPA-Cre and *Twist1*$^{del/+}$; Tyr-Cre mice were mated with *Twist1*$^{3loxPneo/3loxPneo}$ mice. Conditional *Twist1*-null embryos of the respective genotype, *Twist1*$^{3loxPneo/del}$; Wnt1-Cre, *Twist1*$^{3loxPneo/del}$; HtPA-Cre and *Twist1*$^{3loxPneo/del}$; Tyr-Cre, were compared to wild-type littermates.

To track the distribution of the *Twist1*-deficient CNC cells, *Twist1*$^{3loxPneo/3loxPneo}$ mice were mated with Z/AP mice and resulting *Twist1*$^{3loxPneo/+}$; Z/AP offspring mated with *Twist1*$^{del/+}$; Wnt1-Cre mice to produce embryos that contained *Twist1*-deficient and alkaline phosphatase (AP)-expressing cells for analysis.

Pups and embryos were genotyped for the 3loxPneo and deleted alleles using primers 114, 115 and 117 (Chen et al., 2007). All Cre transgenes were detected using the following primers: 5′-CTGACCG-TACACCAAAATTTGCCTG-3′ (CreF), 5′-GATAATCGCGAACATCTTCA-GGTTC-3′ (CreR). Genotypes of Z/AP mice were determined by staining for β-galactosidase activity in samples of ear tissue, or by PCR using the following primers: 5′-TTATCGATGAGCGTGGTGGTTATGC-3′ (lacZ-F) and 5′-GCGCGTACATCGGGCAAATAATATC-3′ (lacZ-R).

Morphometric measurements

Frontal views of the heads of E10.5 Wnt1-Cre CKO, Tyr-Cre CKO embryos and corresponding wild-type specimens were taken at 40× magnification. The width of the forebrain vesicle and the thickness of the nasal tissue mass were measured on digital images using tools in Adobe Photoshop.

Staining for bone and cartilage

Dissected heads of E17.5 embryos were stained with alizarin red and alcian blue to reveal the bone and cartilage respectively (Hogan et al., 1994). Stained specimens were washed, stored and photographed in aqueous 20% glycerol:20% ethanol solution.

Histology

Heads of wild-type and mutant embryos at E15.5 and 17.5 were fixed in 4% paraformaldehyde (PFA) at 4 °C for more than 16 h, washed in PBS for 2 h at room temperature and then washed in H_2O for at 2–6 h at room temperature. The heads were dehydrated through a series of increasing ethanol concentrations (65%–100%) for 1 h each. After dehydration heads were incubated three times for 1 h in xylene and then wax impregnated at 60 °C three times for 1 h in a vacuum oven (Labec). The embedded heads were sectioned on a microtome (RMC MT-920) at 9 μm thickness. Sections were dried overnight and stained with eosin and haematoxylin.

Embedding of tissue for cryosectioning

Heads of E15.5 embryos were collected in PB1, rinsed in PBS (without calcium and magnesium) and fixed in 4% PFA and stored at 4 °C. The heads were then rinsed three times in PBS and dehydrated in 30% sucrose in PBS overnight at 4 °C. Embedding was performed in equal volumes of 30% sucrose/PBS and OTC embedding medium (Tissue Tek). Sections were cut at 14–16 μm on a cryostat (M1900, Leica), collected on Superfrost Plus slides (Menzel-Glaser) and stored at −20 °C.

Alkaline phosphatase staining of cryosections

Slides were warmed to room temperature and rehydrated in PBS for 5 min, fixed in 4% paraformaldehyde for 10 min and rinsed three times in PBS. To inactivate the endogenous alkaline phosphatase the slides were incubated at 70 °C for 30 min, followed by three rinses in PBS and two 10 min incubations in NTMT (0.1 M NaCl, 0.1 M pH 9.5, 0.1 M $MgCl_2$, 1% Tween20). The color reaction was performed using NBT/BCIP or BM Purple (Roche) and specimens mounted in Ultra-mount No.4 (Fronine).

Whole mount alkaline phosphatase staining

Embryos were collected in PB1, rinsed in PBS and then fixed for 2 h in 4% PFA at 4 °C. Two alternative staining protocols were followed. In the first, embryos were rinsed twice in PBS and then washed in 70% ethanol for 2–16 h at 4 °C. The embryos were then transferred to PBS/0.1% Tween-20. Inactivation of endogenous AP and color development was performed as described above for cryosections. Alternatively, embryos were fixed in glutaraldehyde as described by Lobe et al. (1999). The embryos were then briefly washed with PBS and endogenous AP inactivated at 70 °C for 30 min. Subsequent steps were as described above.

Whole mount in situ hybridization

For in situ hybridization, the initial steps prior to prehybridization were carried out manually following established protocols (Henrique et al., 1995) except that prehybridization was performed in 5×SSC, 50% formamide and 1% SDS. This was followed by automated processing and hybridization (InsituPro, Intavis AG) as described previously (Loebel et al., 2004). Post-hybridization washes were carried out in

50% formamide, 5×SSC and 1% SDS, and specimens were stained with BM Purple. Riboprobes for whole mount in situ hybridization on E10.5 or E11.5 mouse embryos were made from plasmid clones containing fragments of the following cDNAs: *Alx3*, *Alx4*, *Cart1*, *Dlx2*, *Dlx5*, *Fgf8*, *Fgf10*, *Lhx7*, *Msx2*, *Sox10*, *Twist1*, *Twist2*. The *Runx2* and *Pou3f3* probes were made by amplifying a fragment of each transcript using the following primers:

5′-TGCAAGAAGGCTCTGGCGTTTAAAT-3′ (*Runx2* ORF-F);
5′-CACCTGCCTGGCTCTTCTTACTGAGA-3′ (*Runx2* ORF-R);
5′-AGCAGACGCCGGACGATGTCTA-3′ (*Pou3f3*-F);
5′-AATCACATCCGCAGCACCCATT-3′ (*Pou3f3*-R).

The amplified fragments were gel purified and re-amplified using primers identical to the first round of amplification, except that the reverse primer contained a T7 promoter sequence at the 5′ end. This product was gel purified and used for riboprobe production. Digoxigenin-labeled riboprobes were synthesized using Ampliscribe (Epicentre Technologies).

TUNEL staining

Embryos were collected at E9.5 in PB1 medium and fixed in 4% PFA. Fixed embryos were dehydrated through an ethanol series, embedded in paraffin wax and sectioned. Cryosections of embryos prepared as described above were also used for TUNEL analysis. Labeling was performed using TUNEL labeling mix and TUNEL enzyme (Roche) according to the manufacturer's protocol.

Immunofluorescent detection of Ki67 and F-actin

E9.5 embryos were collected in PB1, rinsed in PBS and fixed in 4% paraformaldehyde. Embryos were embedded and cryosectioned as described above. Slides were stored at −20 °C until required and then fixed in 4% paraformaldehyde for 5 min, rinsed three times in PBS and incubated in blocking buffer (PBS plus 0.02% triton, 1% goat serum and 10% FCS) for 1 h at RT. Primary antibody (rabbit anti-Ki67, Abcam) was added to blocking buffer at 1/100 dilution and slides were incubated and room temperature for 90 min. Slides were then washed with PBS plus 0.02% Triton X-100 three times for 5 min each and then incubated with a goat anti-rabbit Alexa 594 conjugated secondary antibody (Invitrogen) diluted 1/500 in blocking buffer for 1–2 h at room temperature. Slides were washed with PBST three times 5 min each stained with DAPI and mounted in DABCO. Images were captured using an Olympus BX51 microscope and SPOT camera. DAPI and Alexa594 labeled nuclei were counted on digital images of the stained sections using MetaMorph software (Molecular Devices). To detect F-actin, frozen sections were washed three times in PBS, permeabilized in 0.2% Triton X-100/PBS, rinsed again and incubated for 30 min in Alexa 543-conjugated phalloidin (Invitrogen) diluted 1/300 in PBS. After washing in three times PBS, sections were mounted in DABCO and photographed.

Results

Temporal and spatial patterns of Cre recombinase activity

The patterns of recombinase activity driven by Wnt1-Cre, HtPA-Cre and Tyr-Cre in the craniofacial tissues were assessed by examining the

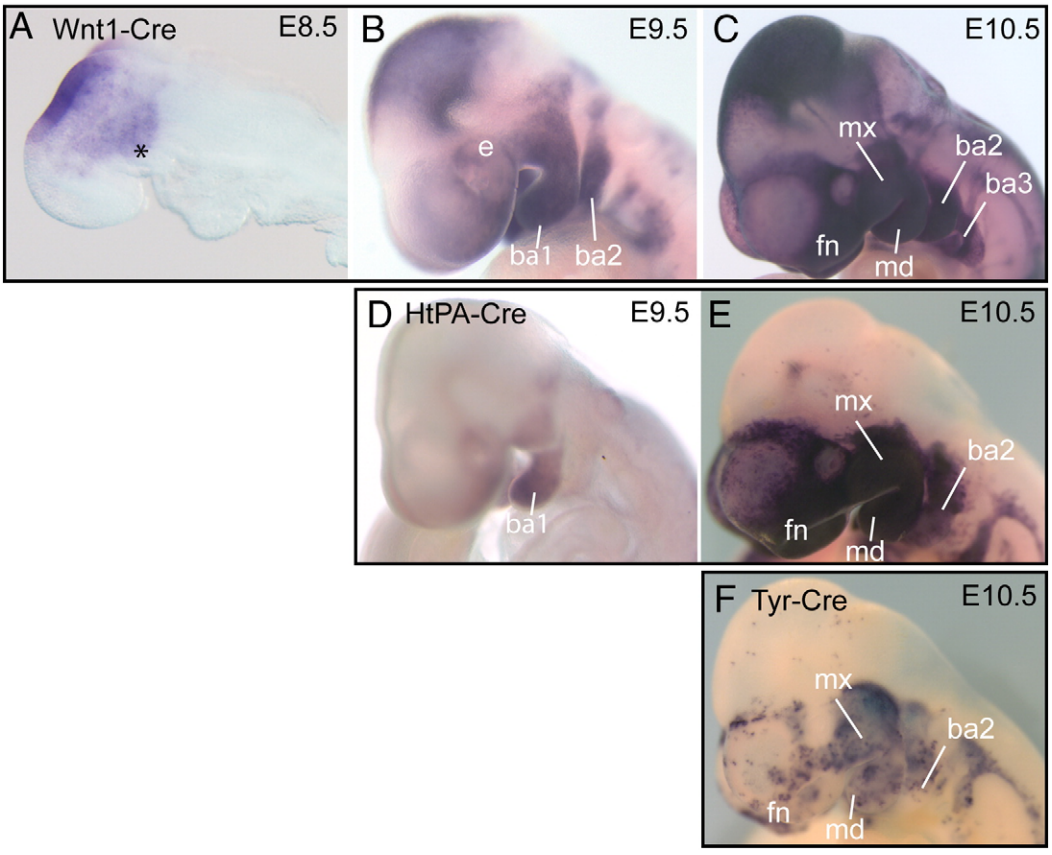

Fig. 1. Cre activity in the craniofacial tissues reported by Z/AP expression. (A–C): Wnt1-Cre×Z/AP embryos at E8.5 (A), E9.5 (B) and E10.5 (C). (D, E): HtPA-Cre×Z/AP embryos at E9.5 (D) and E10.5 (E). (F): Tyr-Cre×Z/AP embryo at E10.5 (F). Abbreviations: ba1, ba2, ba3: first, second and third branchial arch; e, eye; fn, frontonasal region; md, mandible; mx, maxilla; * base of ba1.

expression of the Z/AP reporter (Lobe et al., 1999). Following excision of upstream loxP-flanked *lacZ* sequences of this reporter construct, human placental alkaline phosphatase (AP) is activated and permanently marks cells that have expressed Cre.

Of the three Cre transgenes, Wnt1-Cre was detected earliest during development (Figs. 1A–C). Wnt1-Cre activity was detected at E8.5 in the neural crest of the midbrain, and in the mesenchyme spanning from the lateral margin of the neural plate to the base of the nascent first branchial arch (Fig. 1A). By E9.5, AP-stained cells populated the mesenchyme in the frontonasal and periocular regions and the first and second branchial arches (Fig. 1B). By E10.5, additional AP-positive cells were found in the nasal prominences, maxillary eminences, and the third branchial arches (Fig. 1C). HtPA-Cre activity was first detected at E9.5, in the mesenchyme of the periocular and nasal region and the first branchial arch (Fig. 1D). By E10.5, in some specimens, AP-positive cells were present in the tissues of the first and second branchial arches, frontonasal and periocular mesenchyme (Fig. 1E) in a pattern similar to that seen in Wnt1-Cre-expressing embryos. However, HtPA-Cre expression varied among the embryos, ranging from a mosaic pattern in the craniofacial tissues to widespread staining throughout the embryo (Supplementary Figs. S1A, B). Activity of Tyr-Cre was not detected at E9.5 (data not shown) but was present by E10.5, after the completion of CNC cell migration. AP-positive cells were found in a punctate pattern in the mesenchyme surrounding the forebrain vesicle and the optic evagination, and in the branchial arch tissues and the nerves and ganglia of the facioacoustic, accessory and vagal nerves (Fig. 1F).

Based on our Z/AP reporter experiments, we expected that Wnt1-Cre would produce the most widespread deletion of *Twist1* in the cranial tissues, with Tyr-Cre resulting in more limited loss. To test this prediction, we compared *Twist1* expression in Wnt1-Cre and Tyr-Cre conditional knockout (CKO) embryos to the wild-type expression pattern (Fig. 2). In Wnt1-Cre CKO embryos at E9.5 or E10.5, no *Twist1* expression was detected in the frontonasal, periocular or branchial arch tissues (Figs. 2A–F). Weak *Twist1* expression remained in the paraxial cranial mesenchyme at E9.5 and E10.5 (Figs. 2B, E, F). Tissues that retained *Twist1* expression in Wnt1-Cre CKO embryos were localized in the region where Mesp1-Cre is expressed (Yoshida et al., 2008), suggesting that they are mesodermal cells. *Twist1* expression was not examined in HtPA-Cre CKO embryos because of the variable nature of Cre expression noted above. In Tyr-Cre CKO embryos, *Twist1* expression was absent in many of the same tissues as in the Wnt1-Cre CKO embryos (Figs. 2G, H). However, residual *Twist1* expression remained in the mesenchyme ventral to the eye, adjacent to the nasal pits and in the distal part of the mandibular process of the first branchial arch. Differences in timing and pattern of Cre expression therefore affect the extent of ablation of *Twist1* in the presumptive CNC derivatives.

Loss of facial and upper jaw precursor tissues

E10.5 $Twist1^{del/del}$ embryos (produced by CMV-Cre excision of the floxed allele) displayed craniofacial malformations and closure defects of the cephalic neural tube (Figs. 3A–D) similar to those in the conventional null mutant (Chen and Behringer, 1995;Chen et al., 2007), suggesting the deleted (del) alleles is functionally null. Compared to wild-type embryos (Figs. 3A, B, I), the frontonasal, sub-ocular and first branchial arch tissues were clearly reduced (Figs.

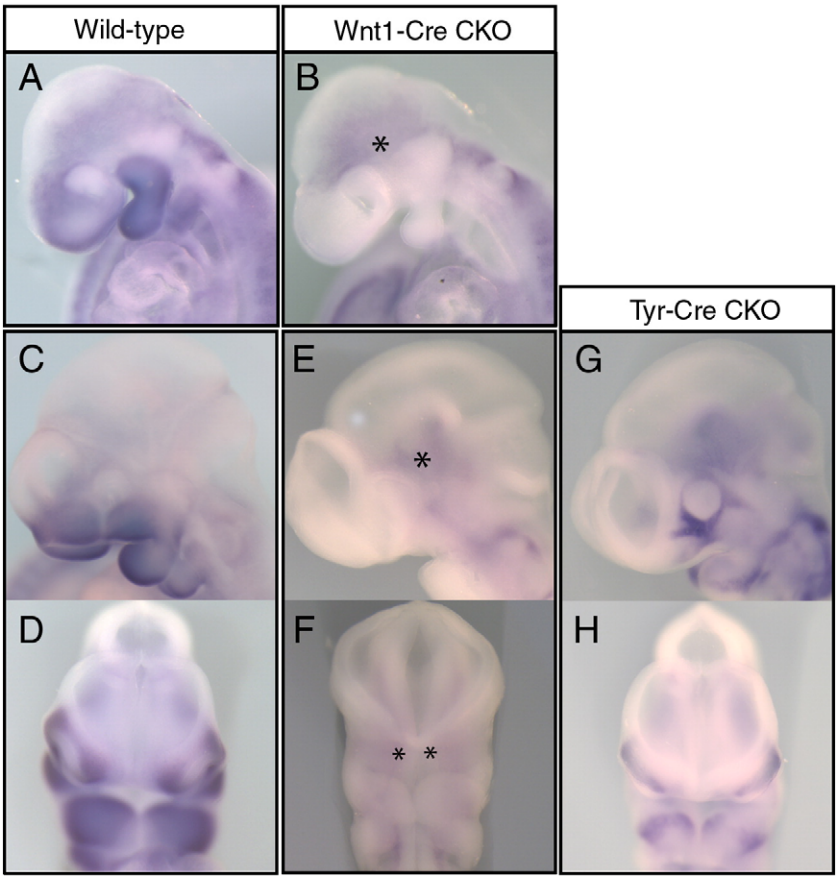

Fig. 2. *Twist1* expression in the craniofacial region in the wild-type embryos (A, C, D), Wnt1-Cre conditional knockout (CKO) embryos (B, E, F) and Tyr-Cre CKO embryos (G, H). *Twist1* in situ hybridization was performed on embryos at E9.5 (A, B) and E10.5 (C–H). In the Wnt1-Cre CKO (B, E, F), no *Twist1* expression was observed in the tissues normally populated by the neural crest cells. Residual expression is found in the mesenchyme adjacent to the brain (asterisks). Some *Twist1* gene expression remains in Tyr-Cre CKO (G, H); notably in the periocular region (G) and the distal part of the first branchial arch (H).

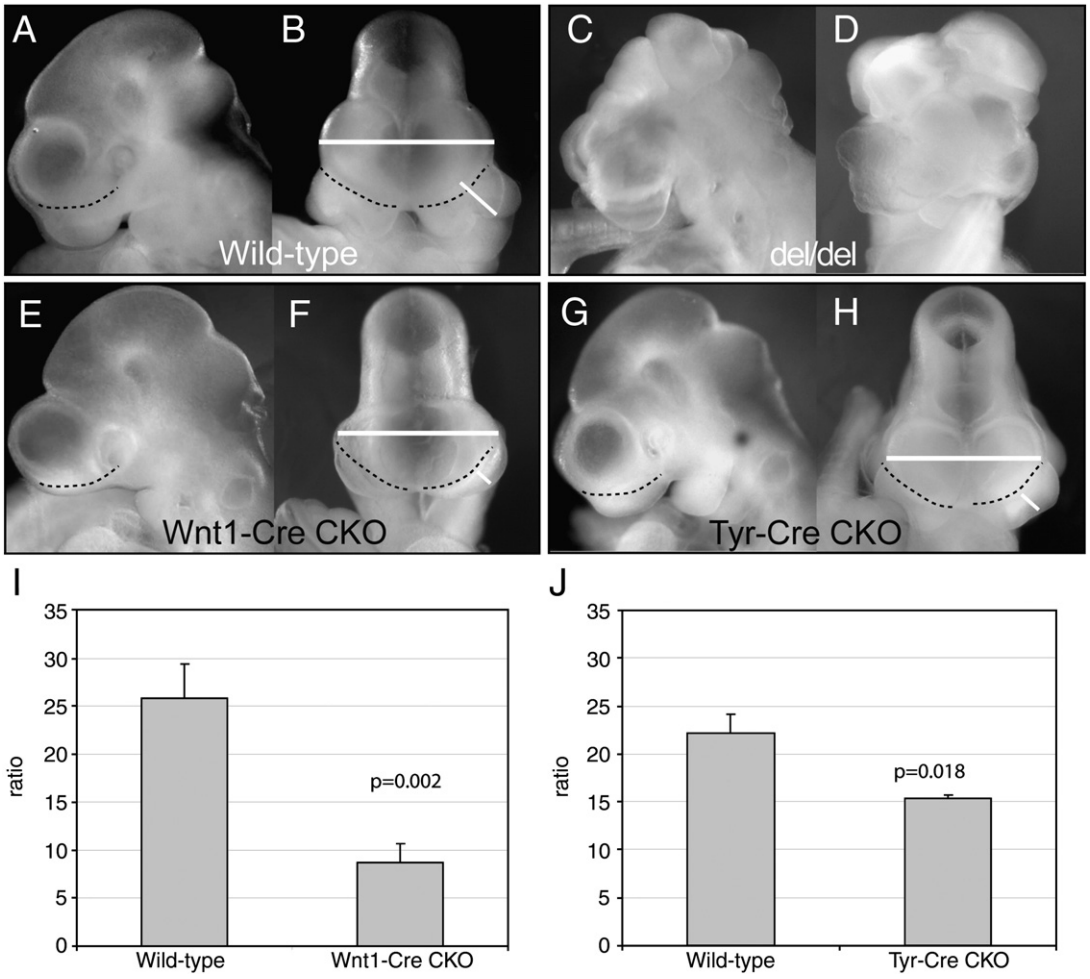

Fig. 3. Head morphology of *Twist1* mutant embryos at E10.5. Wild-type (A, B) and *Twist1*-null (del/del) (C, D) embryos were compared to Wnt1-Cre CKO (E, F) and Tyr-Cre CKO embryos (G, H). Lateral views (A, C, E and G) and frontal views (B, D, F and H). The dashed lines mark the base of the forebrain. (I, J) Significant reduction in the mass of frontonasal tissues in Wnt1-Cre and Tyr-Cre CKO embryos. Quantification of tissue mass was determined by measuring the ratio of the thickness of the nasal tissue (oblique bars) to the width of the forebrain vesicle (horizontal bars). Data are presented as mean and SEM. Significant difference between wild-type and CKO embryos by two-tailed *t*-test at the *p* value indicated. Number of samples = 5 for each group. Somite numbers of the embryos are not different between groups: Wnt1-Cre wild-type = 36.4 ± 0.5, Wnt1-Cre CKO = 37.2 ± 1.5; Tyr-Cre wild-type = 35.0 ± 3.4, Tyr-Cre CKO = 36.0 ± 0.9.

3E, F, I). However, in contrast to the *Twist1*$^{del/del}$ embryos, the cranial neural tube of Wnt1-Cre CKO embryos was closed at E10.5. In the Tyr-Cre CKO embryos, there was a lesser reduction in the frontonasal tissue mass (Figs. 3G, H, J). Consistent with the variable loss of *Twist1* activity, HtPA-Cre CKO embryos displayed a wide range of abnormalities from a modest reduction in frontonasal and first branchial arch tissues to extensive cranial malformations that are reminiscent of that of *Twist1*-null embryos (Supplementary Figs. S1C, D).

To further examine the ontogeny of this phenotype we analyzed the phenotypes of embryo heads collected between E11.5 and E14.5. At E11.5 severe reductions in the maxilla, mandible and frontonasal processes were evident in Wnt1-Cre CKOs (Supplementary Figs. S2A–D). By E13.5 and E14.5, the failure to develop much of the upper jaw and cranial vault was evident, and the brain was not covered by any skeletal elements (Supplementary Figs. S2E–J).

We next examined the fate of *Twist1*-deficient cells (identified by AP expression after the recombination of the Z/AP reporter) in Wnt1-Cre CKO embryos. The presence of AP-positive cells in the frontonasal, facial and branchial arch regions of the embryo indicates that *Twist1*-deficient CNC cells were able to reach their destinations by E9.5 and they were widely distributed and not sequestered to any sites in the branchial arch (Figs. 4A, B). However by E10.5, noticeably fewer AP-positive cells were found in the frontonasal and periocular regions (Figs. 4C, D) and by E11.5, AP-positive cells were very sparse in the maxillary and frontonasal tissues (Figs. 4E, F). In contrast, AP-positive cells were found in the mandible at E10.5–E11.5, indicating the presence of viable CNC cells in this embryonic structure (Figs. 4C–F).

To determine the cellular defects underpinning the reduction in tissue mass, we examined cell death by TUNEL staining and proliferation by immunofluorescent detection of Ki67 in the developing craniofacial primordia of Wnt1-Cre CKO embryos at E9.5, prior to the manifestation of major tissue loss. In Wnt1-Cre CKO embryos, more TUNEL-positive cells were detected in the sub-ectodermal mesenchyme where the CNC-derived cells are located; and in the mesenchyme of the first branchial arch than in the wild-type embryo (Figs. 4G–J). Nile blue staining of whole embryos for detecting necrotic cells also revealed stronger staining of the frontonasal mesenchyme of the CKO embryos (Fig. S3), which is consistent with an increase in cell death in this tissue associated with loss of *Twist1* activity.

Examination of Ki67 immunofluorescence revealed strongly fluorescent cells in the cranial mesenchyme of the wild-type embryos and the CKO embryos (Figs. 4K, L). Ki76-positive cells were present in 4.8% (±0.59, $n = 4$) and 5.1% (±0.83, $n = 4$) of the total population of frontonasal mesenchymal cells in the wild-type and CKO embryos respectively. Conditional loss of *Twist1* in neural crest cells therefore does not impact on proliferative activity. A similar level of Ki67 staining was seen in the neuroepithelium of the forebrain and the

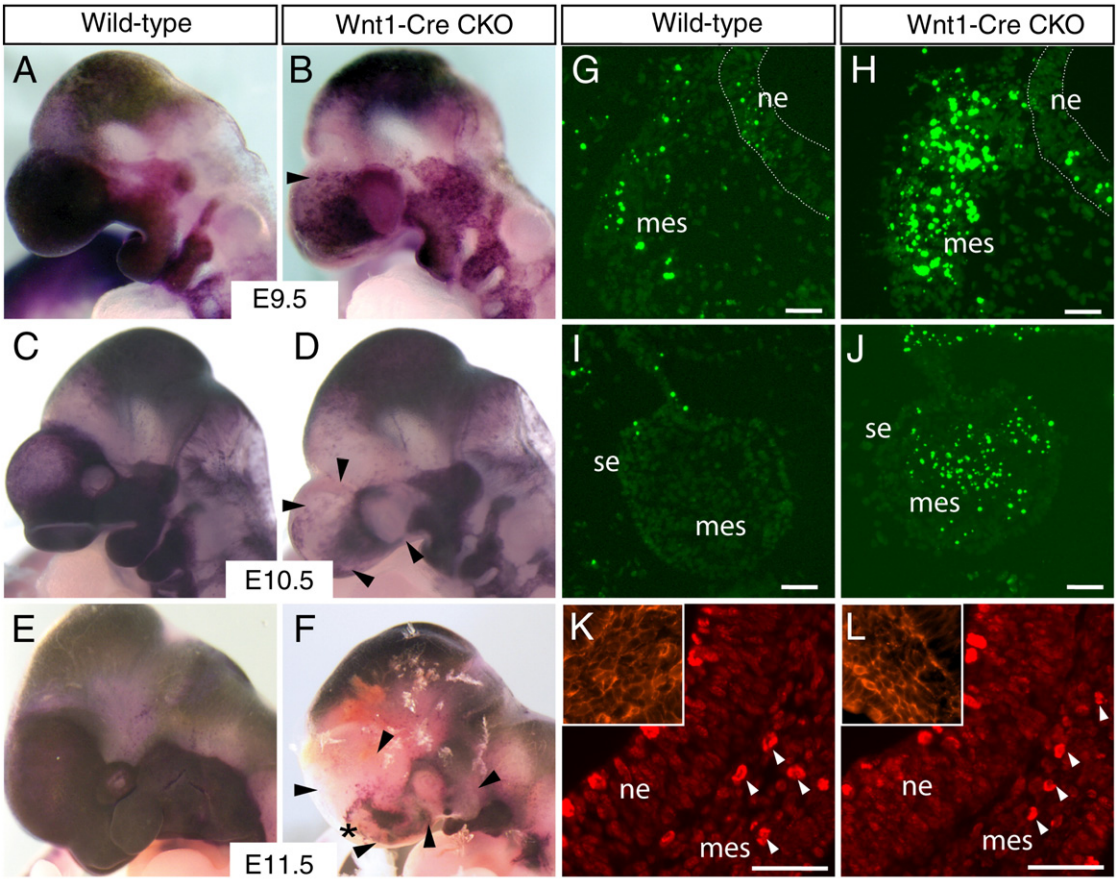

Fig. 4. Fate of neural crest-derived cells in wild-type and Wnt1-Cre CKO embryos. (A–F): Distribution of alkaline phosphatase (AP)-stained cranial neural crest cells in wild-type (A, C and E) and Wnt1-Cre CKO embryos (B, D and F) at E9.5 (A, B), E10.5 (C, D) and E11.5 (E, F). In the E9.5 CKO embryo (B), fewer AP-positive cells are present in the frontonasal, maxillary and mandibular regions compared with the wild-type embryo (A). The loss of AP-positive cells from the frontonasal region is exacerbated in the E10.5 (D) and E11.5 (F) CKO embryos, while the mandible still contains AP-positive cells. Black arrowheads in B, D, F mark regions with reduced numbers of AP-stained cells. (G–J): TUNEL staining of coronal sections of the craniofacial region reveals increased cellular apoptosis in the sub-ectodermal frontonasal mesenchyme (G, H) and mandibular arch (I, J) of Wnt1-Cre CKO embryos (H, J) compared to wild-type (G, I). White dotted lines outline the neuroepithelium. (K, L): Ki67 immunofluorescence of the frontal section of the head region showing proliferating mesenchymal cells (white arrowheads) in the wild-type (K) and CKO (L) embryos at E9.5. Insets show similar morphology and packing density of mesenchymal cells of wild-type and CKO embryos revealed by phalloidin staining of F-actin. Abbreviations: mes, mesenchyme; ne, neuroepithelium; se, surface ectoderm. Scale bar = 50 μm.

surface ectoderm of the wild-type and mutant embryos, suggesting that cell proliferation is also unaffected in tissues that do not normally express *Twist1*. Both the packing density of mesenchymal cells in frontonasal region (number of cells/mm^2: wild-type = 7379 ± 695, CKO mutant = 7271 ± 702, $n = 4$ for each genotype) and the morphology (revealed by phalloidin staining, Figs. 4K, L insets) were not affected by the loss of *Twist1* activity. These results indicate that the reduction of frontonasal and periocular tissue mass in Wnt1-Cre CKO embryos is due primarily to the effects of cell death, and not changes in the cell proliferative activity or tissue architecture.

Loss of Twist1 impairs differentiation of CNC derivatives

In Wnt1-Cre CKO embryos, some *Twist1*-deficient CNC cells remained in the branchial arches and frontonasal tissues, as revealed by AP staining. To investigate the differentiation potential of the *Twist1*-deficient tissues in Wnt1-Cre CKO embryos, markers of CNC differentiation were examined. In wild-type embryos, *Sox10* is expressed in migratory neural crest cells and is down-regulated in post-migratory CNC cells as they undergo non-neurogenic differentiation (Figs. 5A, C; Soo et al., 2002). In CKO embryos, *Twist1*-deficient cells in the frontonasal, periocular and maxillary regions retained strong *Sox10* expression, but cells in the distal parts of the mandibular prominence of first branchial arch appeared to down-regulate *Sox10* (Figs. 5B, D). Loss of *Twist1* therefore seems to disrupt the differentiation of neural crest cells except for those in the distal part of mandible. We further examined CNC differentiation by analyzing the expression of *Msx2*, an early marker of the CNC-derived osteogenic lineage (MacKenzie et al., 1992) and *Runx2*, which is critical for bone differentiation (Komori et al., 1997). At E10.5, *Msx2* is normally expressed in the precursors of the mandible, the maxilla, the nasal and frontal bone (Fig. 5E). In CKO embryos, *Msx2* was expressed in the mandible but not the maxilla (Fig. 5F). *Runx2*, which is expressed in the mandible, maxilla and frontonasal regions of E11.5 wild-type embryos (Fig. 5G), was only weakly expressed in the maxilla and mandible of CKO embryos (Fig. 5H). *Twist1*-deficient frontonasal tissues also failed to express *Alx3* and *Alx4* (Figs. 5I–L), which are essential for normal frontonasal development (Beverdam et al., 2001), and *Dlx5* was absent from the mesenchyme around the nasal placodes (Figs. 5U, W). These findings suggest that the remaining *Twist1*-deficient cells in the frontonasal region of Wnt1-Cre CKO embryos are compromised in their ability to undergo skeletal differentiation. In contrast, *Alx3* expression was retained in the frontonasal tissues of Tyr-Cre CKO embryos (Supplementary Figs. S4A, B), which is consistent with the later deletion and less severe malformations in these embryos.

Loss of *Twist1* had different effects on gene expression in the mesenchymal precursors of the maxilla and different parts of the mandible. *Pou3f3* expression in the maxillary prominence and the proximal part of the second branchial arch was absent in Wnt1-Cre CKO embryos (Figs. 5M, N). In the maxillary region, *Lhx7* expression was greatly reduced but was retained in the distal mandible (Figs. 5O, P). In Tyr-Cre CKOs embryos the maxillary and mandibular expression

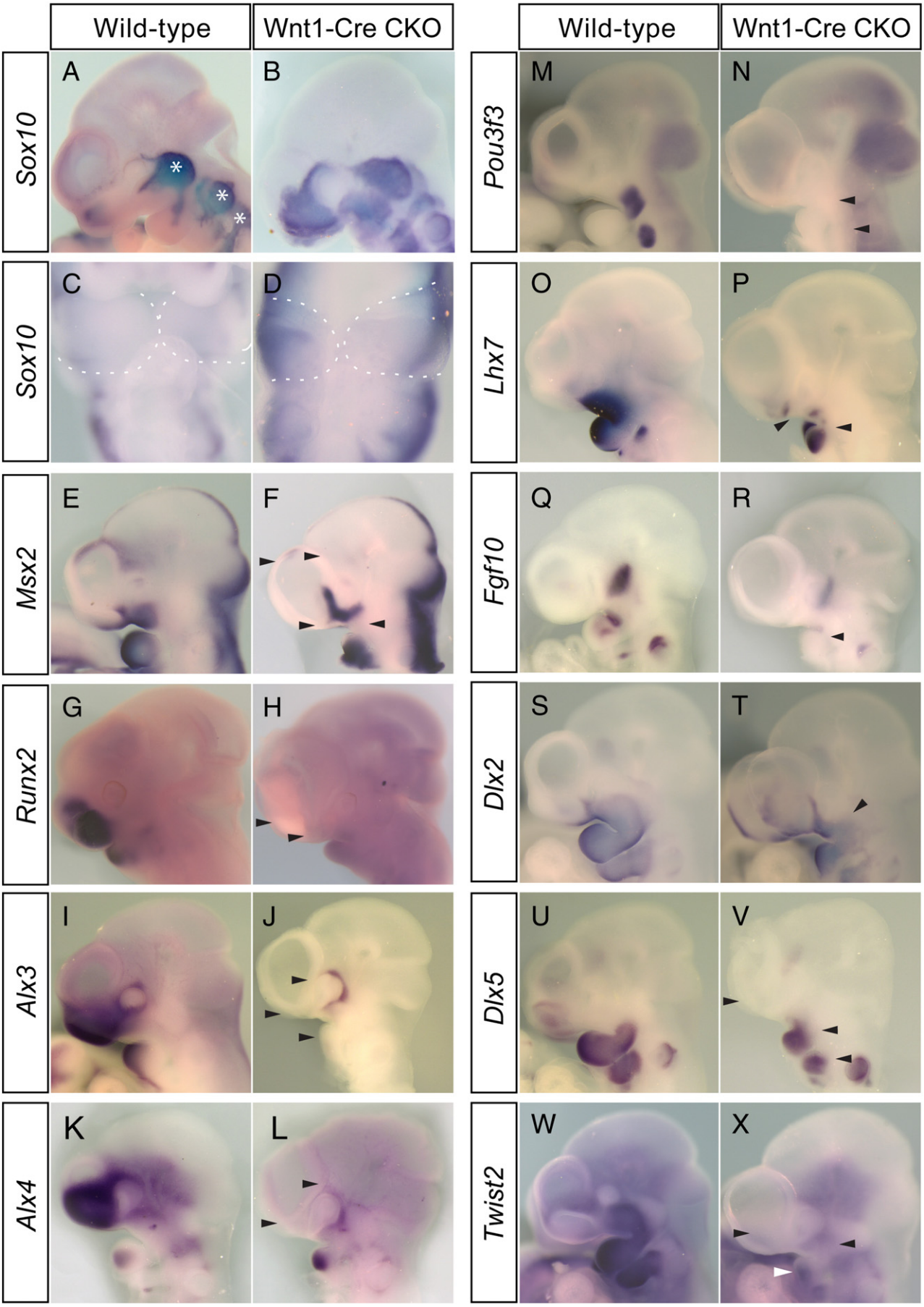
Wild-type
Wnt1-Cre CKO
Sox10
A
B
Sox10
C
D
Msx2
E
F
Runx2
G
H
Alx3
I
J
Alx4
K
L
Wild-type
Wnt1-Cre CKO
Pou3f3
M
N
Lhx7
O
P
Fgf10
Q
R
Dlx2
S
T
Dlx5
U
V
Twist2
W
X

domains of *Lhx7* merged together, consistent with a loss of proximal tissue in the mandible (Supplementary Figs. S4C, D). *Fgf10* expression was lost from the angle between the maxilla and mandible (Figs. 5Q, R). The domain of expression of *Dlx2* was reduced in the maxilla and proximal mandible (Figs. 5S, T) and *Dlx5* expression was lost from the proximal parts of the first and second branchial arches (Figs. 5U, V). Not all genes were equally affected within a structure. In the distal part of the mandible of Wnt1-Cre CKO embryos, *Alx3* expression was completely lost whereas *Alx4* expression was maintained (Figs. 5I–L). *Twist2* expression, which overlaps with *Twist1* in the developing first branchial arch in wild-type embryos, was retained in the distal tip of the mandibular arch (Figs. 5W, X). Overall, our data show that loss of *Twist1* expression leads to reduced or lost expression of differentiation markers from the precursor tissues of the frontonasal skeleton, the maxilla and the proximal part of the mandible.

Defects in facial and cranial vault development

To assess the impact of loss of *Twist1* function on craniofacial development, head morphology and skeletal development of late-term CKO embryos were examined. At E17.5, Wnt1-Cre CKO embryos made up 38.5% (13/34) of the litters (25% expected), indicating that there was no early embryonic lethality. The Wnt1-Cre CKO embryos did not develop frontal and upper face structures. The vault of the skull was missing (Figs. 6A–D) and no frontonasal skeleton or upper jaw was formed. The lower jaw was foreshortened, but the tongue developed to nearly the normal size and protruded beyond the mandible. There were no mid-facial structures, and no skeleton covering of the brain (Figs. 6C, D). Ablation of *Twist1* activity at a later developmental stage by Tyr-Cre resulted in a less severe phenotype, with the formation of more skeletal structures in the frontonasal and jaw areas and the occipital parts of the head; and more substantial soft tissue covering the brain (Figs. 6E, F). Rudimentary structures were present in place of the upper jaws and were decorated with vibrissae that are characteristic of more distal premaxillary structures (Fig. 6E).

The phenotypes of CKO embryos were further assessed for bone and cartilage development by alizarin red and alcian blue staining. In E17.5 Wnt1-Cre CKO embryos, the entire frontal bone and the supraoccipital bone of the skull were absent. Only a thin rim of ossified tissue corresponding to remnants of the parietal and interparietal bones was present (Figs. 6G–J). Formation of the skull in Tyr-Cre CKO embryos was also disrupted, but more substantial development of skeletal elements was evident, such as the parietal and interparietal bones and a thin fragment of bone anterior to the parietal bone, which is possibly a remnant of the frontal bone (Figs. 6K, L). At the base of the skull, the basisphenoid was severely reduced in Wnt1-Cre CKO mutants and development was truncated anterior to this point (Fig. 6J). In Tyr-Cre CKO mutant the basisphenoid developed normally (Fig. 6L)

The upper jaws and frontonasal skeleton were severely affected in CKO embryos. In Wnt1-Cre CKO embryos the frontonasal skeleton was absent and laterally protruding bony structures were formed in place of the maxillae and premaxillae (Figs. 6I, J). Unlike maxillae or premaxillae, these bony rudiments encased cartilaginous rods giving an appearance reminiscent of the lower jaw. However, we saw no evidence for jaw transformation in our study of gene expression in E10.5 embryos (Fig. 5). In Tyr-Cre CKOs, more nasal cartilage was present, along with fragments of bone in the position of the premaxilla and protruding bony rudiments that enveloped a cartilaginous element in place of the maxilla (Fig. 6L). This suggests that the cartilaginous rod in the Wnt1-Cre CKOs may be the remnant of nasal cartilage which has been incorporated into bony structures formed in the place of the maxilla and/or premaxilla. No recognisable primary or secondary palate, normally associated with the premaxilla and maxilla, were formed in any of the CKO mutant embryos.

In Wnt1-Cre and Tyr-Cre CKO embryos, the dentary bones were truncated at the distal end and they did not fuse (Figs. 6J, L). In contrast, Meckel's cartilage, although shortened (Figs. 6I, K), fused at the distal end. The lower jaw was also truncated at the proximal end. The condyloid process and angle were absent and there was no articulation with the skull. Meckel's cartilage did not extend into the otic region (Figs. 6M–O). The tympanic ring was absent and, although there were cartilaginous structures in the otic region, they did not form recognizable primordia of the incus, malleus or styloid process in Wnt1-Cre or Tyr-Cre CKO mutants (Figs. 6M–O).

The phenotypes of HtPA-Cre CKO embryos were more variable, ranging from only a cleft face to a more extreme form with a fully exposed brain and hypoplastic jaws (Supplementary Figs. S1E, F, I–L). Fewer than expected (25%) HtPA-Cre CKO embryos were recovered at E17.5 (8.8%, $n=34$). The craniofacial skeleton displayed varying degrees of loss of elements, mainly those in the skull vault and the mid-facial region (Supplementary Figs. S1G, H, M. N).The variable head phenotype is consistent with the variable expression of the HtPA-Cre revealed by AP reporter staining (Supplementary Figs. S1A, B), which is expected to lead to different degrees of *Twist1* deficiency.

Different impact on facial/upper jaw versus lower jaw structures

Histological analysis, which revealed the extent of the loss of craniofacial tissues, was performed only on Wnt1-Cre CKO embryos in view of the consistency of the mutant phenotype. The CKO embryo displayed major malformation of the brain and loss of skull and upper jaw structures (Figs. 7A, B). Although the mandible was formed, the body had less lateral and dorsal bone mass. Teeth were formed in the truncated lower jaws. Morphologically normal incisor primordia were present at the distal region of the mandible (Figs. 7C, D). By E17.5 two sets of upper and lower molars were present in wild-type embryos (Fig. 7E) and in mutant embryos, the first set of lower molars was at a comparable stage of development to wild-type counterparts, but was smaller and oriented outwardly (Fig. 7F). The second set of lower molars was absent (data not shown), presumably associated with the proximal truncation of the mandible. No upper molars or incisors were formed in the rudimentary upper jaw-like structure (data not shown). The tongue was attached to a wide area on the floor of the lower jaw and was disproportionally large for the jaw (Fig. 7F). The submandibular and sublingual ducts were absent, suggesting the salivary glands were not formed.

To examine the cellular composition of the lower jaw, we performed AP staining of tissue sections from E15.5 Wnt1-Cre CKO

Fig. 5. Expression of tissue markers in the wild-type and Wnt1-Cre CKO embryos analyzed by in situ hybridization at E10.5 (A–F, I–X) and E11.5 (G, H). *Sox10* (A–D) is down-regulated in the non-neurogenic cells in the branchial arches and frontonasal tissues but expression persists in the precursors of the cranial nerve ganglia (asterisks) of wild-type embryos (A, C) but *Sox10* expression is retained in the tissues of the frontonasal and proximal first arch regions (B), and is down-regulated in the distal mandibular region of the first branchial arch (frontal view, D) of the CKO embryos. Broken lines outline the mandible. *Msx2* (E, F) expression is lost from the maxilla and nasal placode in CKO embryo. *Runx2* (G, H) is normally expressed in the mandible, maxilla and frontonasal tissues at E11.5 (G), and is weakly expressed in the mandible and maxilla of CKO embryo (H). *Alx3* expression (I, J) is lost from the frontonasal and mandibular tissues in CKO embryos (J). *Alx4* expression (K, L) is lost in the frontonasal region, but retained in the distal part of the mandible of CKO embryo (L). *Pou3f3* expression (M, N) marks the maxilla and proximal part of the second branchial arch in wild-type embryo (M), but its expression is completely absent in CKO embryo (N). *Lhx7* (O, P) is expressed in the maxilla and distal part of mandible of the wild-type embryo (O), and is retained in the mandible of CKO embryo (P). *Fgf10* expression (Q, R) at the angle of the mouth between the maxilla and mandible (Q) is lost in CKO embryo (R). *Dlx2* (S, T) is normally expressed in the first and second branchial arches (S) and shows a reduced domain of expression in CKO embryo (T). *Dlx5* expression (U, V) in the mandible and the second branchial arch is retained only in the distal part of the arches in the CKO embryo (V). *Twist2* expression (W, X) is maintained weakly in the distal part of the mandible of the CKO embryo (white arrowhead in X). Black arrowheads indicate regions where expression is lost or significantly reduced in CKO embryos.

embryos carrying the Z/AP reporter. As previously observed (Abe et al., 2007) Wnt1-Cre directs widespread reporter expression in the lower jaw, including the dentary bone and Meckel's cartilage. Staining was evident in wild-type and CKO tissues, indicating that that the dentary bone and Meckel's cartilage contained cells of CNC origin (Figs. 7G, H).

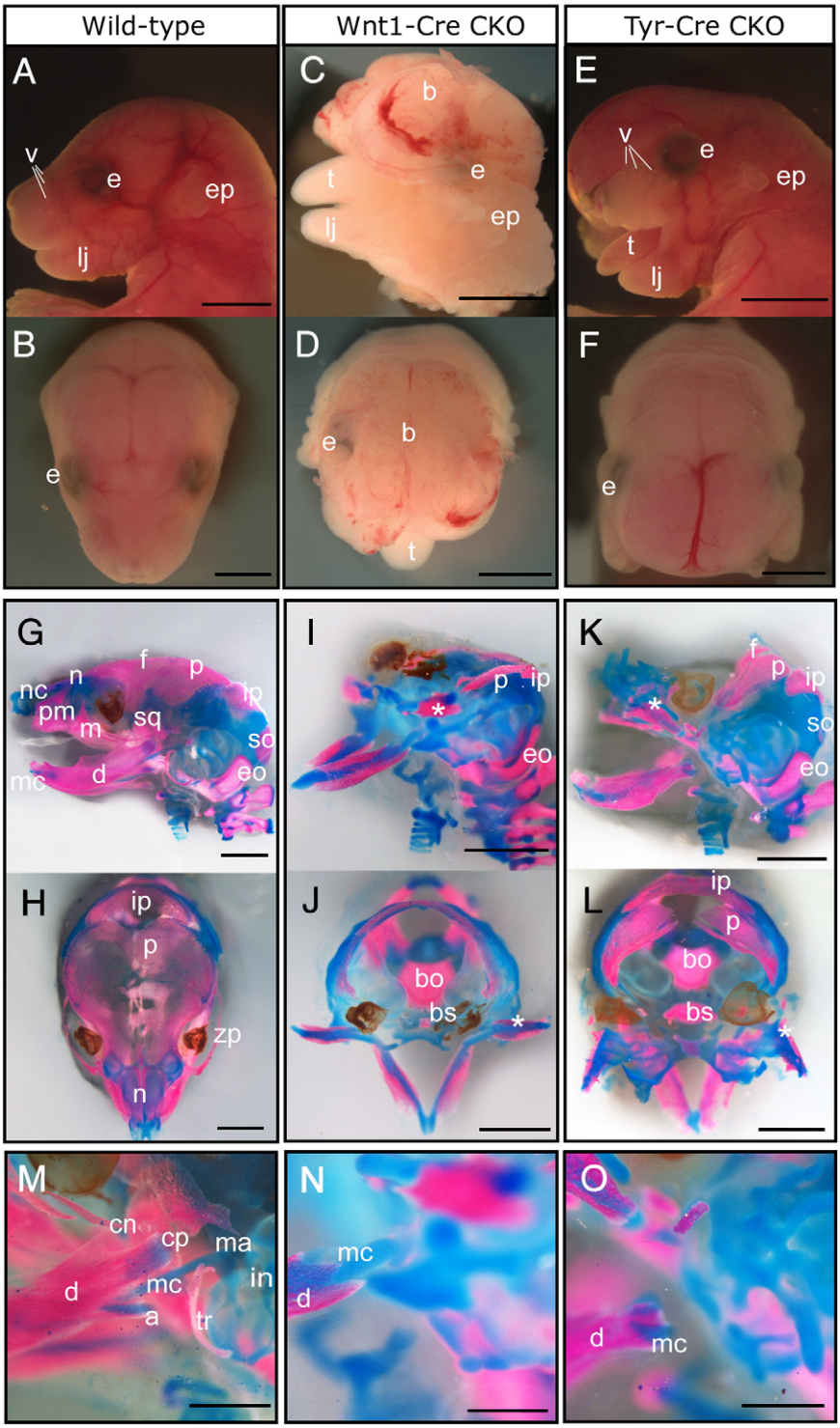

Fig. 6. (A–F): Craniofacial morphology of CKO mutant embryos at E17.5. Morphology of the head of E17.5 wild-type (A, B), Wnt1-Cre (C, D) and Tyr-Cre (E, F) CKO embryos. (A, C, E) Lateral views and (B, D, F) dorsal views. The mutants lost the skull and frontonasal tissues and have a rudimentary structure in place of the upper jaw. In the Wnt1-Cre CKOs the brain (b) is exposed and the lower jaw (lj) is truncated with a protruding tongue (t). The eye (e) and ear pinna (ep) are displaced. In the Tyr-Cre specimen the skin over remnant of upper jaw is decorated with vibrissae (v). (G–O): Alizarin red and Alcian blue staining of the skeleton in the head of wild-type embryos and Wnt1-Cre and Tyr-Cre CKO embryos at E17.5: Lateral (G–K, M–O) dorsal (H–L) views. M–O shows higher magnification views of the proximal jaw and otic region. In the CKO embryos, several skeletal elements of the nasal structure and the skull vault were either missing or reduced: e.g. premaxilla (pm), maxilla (m), nasal (n), frontal (f) squamosal (sq) and supraoccipital (so). In the lower jaw, Meckel's cartilage (mc) and the dentary (d) bone are both present but truncated. The coronoid (cn) and condylar (cp) processes and angle (a) are absent in CKOs and Meckel's cartilage does not extend into the otic region, which lacks the tympanic ring (tr), incus (in) and malleus (ma) (M–O). A protruding rudiment is present in place of the maxilla (asterisk) in CKO mutants. Scale bars: (A–F) 3 mm, (G–L) 4 mm, (M–O) 2 mm. Other abbreviations: bo, basioccipital; bs, basisphenoid; eo, exoccipital; ip, interparietal; nc, nasal capsule; p, parietal; zp, zygomatic process.

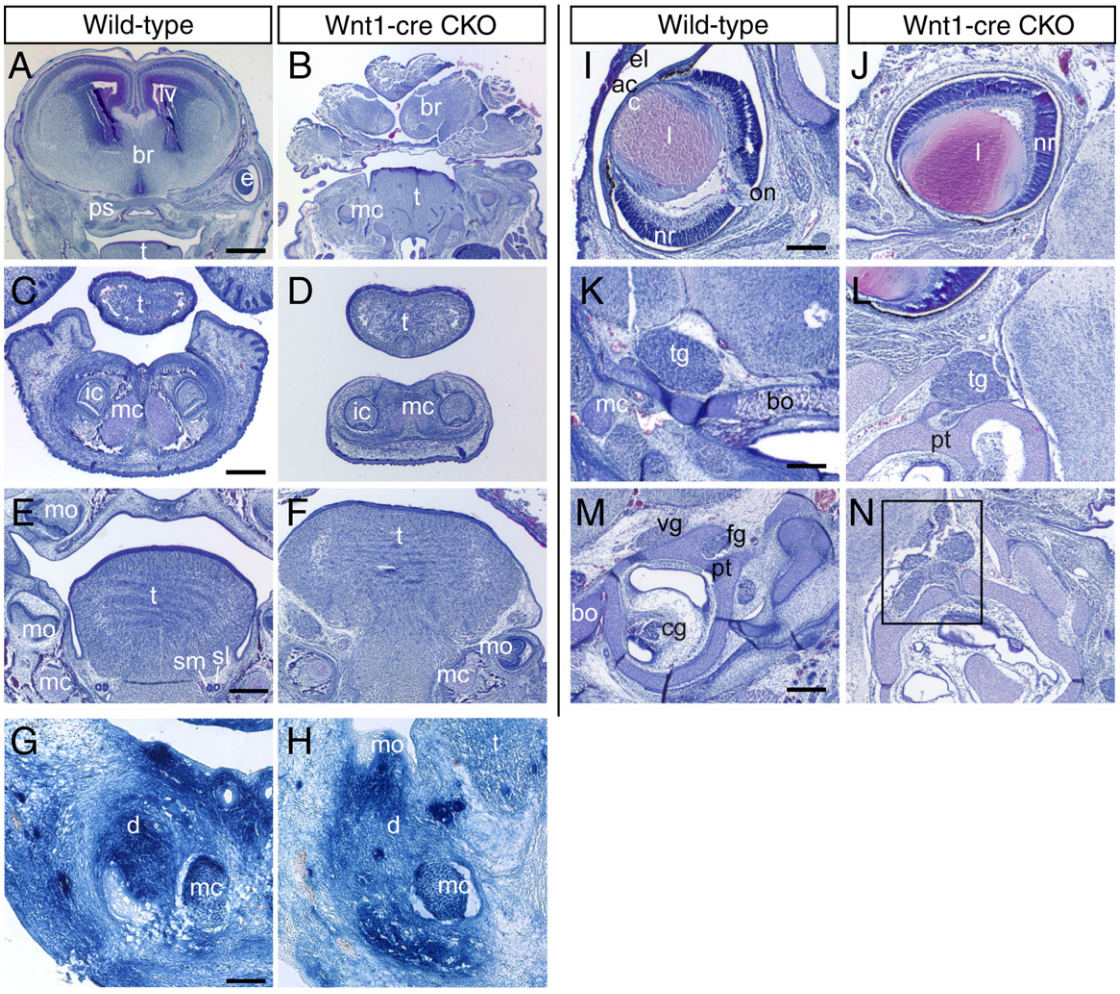

Fig. 7. Histology of wild-type and Wnt1-Cre CKO embryos. Sections through the upper part of the head (A, B) reveal the absence of skull and soft tissue over the brain (br). The distal lower jaw contains the incisors (ic) (C, D) and the first set of lower molars (mo) (F), which although appeared small, have developed to the stage comparable to those in the jaws of the wild-type embryo (E). The submandibular (sm) and sublingual (sl) ducts are absent in the CKO embryo. In the E15.5 wild-type (G) and Wnt1-Cre CKO embryo (H), alkaline phosphatase-positive tissues are present in the dentary bone (d) and Meckel's cartilage (mc). In E17.5 CKO embryos (I, J), eyes were buried in soft tissue and inappropriately oriented. The cornea (c), the anterior chamber (ac) and the optic nerve (on) were missing. The trigeminal ganglion (tg) is shifted caudally to near the otic capsule (K, L) and juxtaposed (box) to the facial (fg) and vestibular (vg) ganglia (M, N). Individual pairs of panels are shown at the same magnification. Other abbreviations: bo, basioccipital; cg, cochlear ganglion; el, eye lid; lv, lateral ventricle; nr, neural layer of retina; pt, petrous part of temporal bone; ps, presphenoid; t, tounge. Scale bar = 200 μm (A, B), 100 μm (C–F, I–M) and 50 μm (G, H).

Overall, the results demonstrate that loss of *Twist1* in the CNC affects the development of bones and cartilages of the skull, the face and upper jaws to varying degrees and the lower jaws are less affected. The similar spectrum of skeletal malformations caused by ablation of *Twist1* at early (Wnt1-Cre) and late (Tyr-Cre) phases of neural crest development highlights a requirement for *Twist1* primarily in post-migratory CNC cells. The findings reveal an essential role for *Twist1* in skeletogenic differentiation of the CNC and point to a differential effect of loss of *Twist1* in the frontonasal and maxillary primordia compared to the mandibular primordium.

Loss of facial skeleton is associated with misplacement of eyes and cranial nerve ganglia

In Wnt1-Cre CKO embryos (Fig. 7I), eyes were formed but, in the absence of supporting skeleton, were displaced caudally and embedded in the tissue of the temporal region. In wild-type embryos the eyes were oriented laterally with the lens facing outward and the optic nerve extending medially towards the brain (Fig. 7J). In CKO mutants, the eyes were incorrectly oriented with the lens facing ventrally. The cornea and the anterior chamber were absent. Optic nerves were absent in E17.5 specimens but were found in some E15.5 mutant embryos (data not shown).

CNC-derived cranial nerves and ganglia were present in Wnt1-Cre CKO embryos, indicating that the CNC was able to undergo neurogenesis. The trigeminal ganglion, although displaced caudally and juxtaposed to the facial and vestibulocochlear ganglia, was formed and was of a similar size to that in wild-type embryos (Figs. 7K–N). Therefore, *Twist1*-deficient CNC cells retain neurogenic capacity but the neural derivatives are not properly patterned.

Discussion

The primary role of Twist1 in the cranial neural crest cells

In this study we have shown that loss of *Twist1* in the CNC lineage results in major defects in the formation of craniofacial skeleton, including a failure to develop much of the skeleton of the face and skull vault (Fig. 8). However, the cranial neural tube initially develops normally and disruption to craniofacial development is less extreme at mid-gestation than that seen in the *Twist1*-null embryos.

We previously observed defects in the migration of the CNC in *Twist1*-null embryos (Soo et al., 2002; Ota et al., 2004) that are not apparent in the CKO mutants. Reciprocal grafting studies suggested that proper CNC migration might require the function of *Twist1* in the mesoderm to facilitate interactions with the

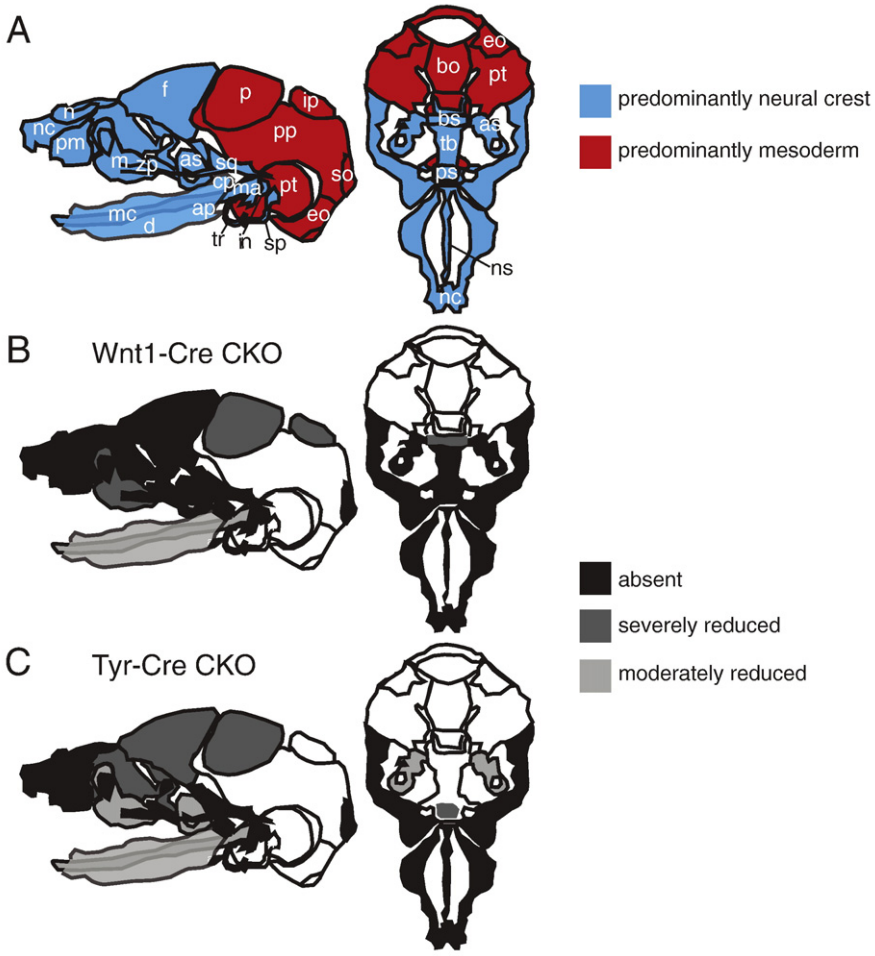

Fig. 8. Formation of neural crest and mesoderm-derived skeletal elements in conditional mutants. (A) Neural crest (blue) and mesoderm (red) contributions to the jaws, face and skull vault (left) and the base of the skull (right). (B, C) Loss or reduction of skeletal elements in Wnt1-Cre CKO embryo (B) and Tyr-Cre CKO embryo (C). Figures. are redrawn based on Depew et al. (2002). Data on neural crest and mesoderm contributions are drawn from several Cre-mediated in vivo lineage tracing studies (Chai et al., 2000; Jiang et al., 2002; Yoshida et al., 2008; McBratney-Owen et al., 2008). Abbreviations: ap, angular process; as, alisphenoid; bo, basioccipital; bs, basisphenoid; cp, condyloid process; d, dentary; eo, exoccipital; f, frontal; in, incus; ip, interparietal; m, maxilla; ma, malleus; mc, Meckel's cartilage; n, nasal; nc, nasal capsule; ns, nasal septum; p, parietal; pm, premaxilla; pp, parietal plate; ps, prespenoid; pt, petrous part of temporal bone; so, supraoccipital; sp, styloid process; sq, squamous; tb, trabecular basal plate; tr, tympanic ring; zp, zygomatic process.

migrating CNC (Soo et al., 2002). In these experiments it was observed that when *Twist1*$^{-/-}$ CNC cells were grafted into wild-type hosts the mutant CNC cells could migrate to the first branchial arch but were not correctly localized. In contrast, when wild-type CNC cells were grafted into a *Twist1*$^{-/-}$ host, the grafted CNC cells were not able to home in to the first branchial arch. In both these experiments the migrating CNC cells were a mixed population consisting of wild-type and mutant cells, so it is not clear whether the observations indicate a disruption in CNC-mesoderm interactions, or a disruption to interactions between CNC cells. In our current study, *Twist1*-deficient CNC cells appear to be distributed widely in the first branchial arch, demonstrating directly that *Twist1* is not required cell autonomously in CNC cells for migration or regionalization. The loss or reduction of a similar set of skeletal elements (Fig. 8B, C) irrespective of whether *Twist1* was deleted early in CNC development (Wnt1-Cre) or after migration (Tyr-Cre) strongly supports the hypothesis that the primary requirement for *Twist1* in the CNC comes after migration is completed.

Twist1 appears to be required in the CNC for cell viability and skeletogenic differentiation. In this study we show an elevated level of cell death in CNC-derived regions. In addition, *Twist1*-deficient CNC cells are unable to progress with differentiation after migration as revealed by the failure to down-regulate *Sox10* and initiate expression of *Msx2*, *Runx2*, *Alx3* and *Alx4* in the maxillary and frontonasal tissues.

Secondary effects of loss of Twist1 function on tissue interactions

Analysis of the skeletal morphology of the head of CKO mutants revealed that CNC-derived skeletal elements are not the only ones affected by the loss of *Twist1* in the neural crest cells. In mice, most of the parietal bones and parts of the interparietal bones are derived from Mesp1-Cre-expressing cranial paraxial mesoderm rather than the Wnt1-Cre-expressing CNC (Fig. 8A) (Jiang et al., 2002;Yoshida et al., 2008). The reduction in the size of the parietal and interparietal bones in CKO embryos suggests that their formation and ossification requires interactions with adjacent neural crest-derived tissues. The meninges underlying the parietal bones, the suture between them and the squamosal bones lateral to them are all predominantly CNC-derived (Yoshida et al., 2008) Similarly, the central portion of the interparietal bone is CNC-derived, as is a patch of dermis rostral to it. The poor development of mesoderm-derived structures that are normally adjacent to CNC structures (Figs. 8B, C) is consistent with previous findings that disrupting the development of the dura either by removal of tissue (Gagan et al., 2007), retinoic acid treatment (Jiang et al., 2002) or loss of *Foxc1* or *Tgfbr2* function (Ito et al., 2003;Vivatbutsiri et al., 2008) perturbs the development of the calvarial bones.

Differential effects of Twist1 ablation in CNC-derived tissues

Although *Twist1* expression is undetectable in CNC-derived tissues in Wnt1-Cre CKO mutants, not all CNC-derived tissues are equally affected by the loss of *Twist1* function (Fig. 8B). The dermal bones of the viscerocranium are derived from the CNC (Morriss-Kay, 2001) and whilst the maxilla, premaxilla, squamosal and zygomatic bones were all missing or severely malformed in CKO embryos, the dentary bone developed and contained teeth. Our data are consistent with the previous finding that when *Twist1*$^{-/-}$ first branchial arch tissue was grafted under the kidney capsule of recipient mice, some capacity to form CNC-derived tissues was retained (Soo et al., 2002).

Our findings clearly demonstrate differential effects of loss of *Twist1* in the CNC in the frontonasal and maxillary processes and the mandibular process. Expression of several genes that we examined was retained in the distal part of the mandible whereas expression of the genes tested in the maxilla and proximal part of the mandible was lost or reduced. This strongly suggests a difference in the requirement for *Twist1* in the CNC of the mandibular process compared to the remainder of the CNC-derived tissues. The basis for this difference is unclear, but may involve a difference in the mode of action of *Twist1* in different regions of the CNC. Differences between early and late migrating CNC cells have been noted previously. In quail-chick grafting experiments, early migrating CNC cells were able to contribute to a wide range of structures including the jaws, whereas late migrating CNC cells did not contribute to the jaws (Baker et al., 1997). The earliest migrating cells are more likely to find their way to the distal parts of the branchial arches, and may be subject to a different signalling environment to the later migrating cells. This difference may underlie the differential requirement for *Twist1* in development of tissues derived from these CNC cell populations.

Another possibility is that the function of *Twist1* might be partially compensated for in the mandible by a related bHLH protein. Both *Twist1* and the closely related *Twist2* are capable of regulating osteoblast differentiation (Bialek et al., 2004) and *Twist2* is expressed in the first branchial arch, overlapping with *Twist1*. Given our observation that expression is maintained, albeit at a low level, in the distal mandible of CKO embryos, it is possible that *Twist2* may partially substitute for *Twist1*. However, major craniofacial abnormalities have not been observed in *Twist1*/*Twist2* compound heterozygous mutant embryos or newborn mice (Sosic et al., 2003 and our unpublished data), revealing no evidence for a genetic interaction in craniofacial development. The finding suggests that compensation for loss of *Twist1* function by *Twist2* is not likely.

Altered bHLH dimerization provides another possible mechanism to explain the differential effects of loss of *Twist1*. *Twist1* is able to form both homodimers and heterodimers with other bHLH proteins, and its activity is in part dependent on its dimerization partner (Castanon et al., 2001). Mutations in residues that regulate *Twist1* dimerization are present in individuals with Saethre-Chotzen syndrome (Firulli et al., 2005). Changes in the level of Twist1 protein in a cell will alter the relative abundance of homodimers and heterodimers involving *Twist1* and its dimerization partners, which will affect the regulation of transcriptional targets (Connerney et al., 2006;Laursen et al., 2007). This has been shown in the development of the cranial sutures, where genes that are regulated by *Twist1* homodimers and heterodimers are expressed at different sites and suture fusion is influenced by the amount of homodimer or heterodimer present (Connerney et al., 2006;Connerney et al., 2008). *Twist1* and *Hand2* are co-expressed in limbs and some craniofacial tissues. *Twist1* and *Hand2* physically interact and it appears that they have antagonistic activities, since reduced *Hand2* expression can overcome the effects of *Twist1* haploinsufficiency and over expression of *Hand2* phenocopies the effects of reduced *Twist1* on limb development (Firulli et al., 2005). It is possible that a similar interaction occurs between *Twist1* and a tissue-specific bHLH factor in the craniofacial tissues. The presence of one or more tissue-specific dimerization partners whose activity is affected by the absence of *Twist1* could explain the differences in the consequences of loss of *Twist1* on development of the face and skull vault as compared to the lower jaw.

Acknowledgments

We thank Robyn Jamieson for advice on the interpretation of the eye phenotype, Christine Smyth for assistance with image analysis, the CMRI BioServices Facility for maintaining the mouse stocks, Sylvie Dufor for the gift of HtPA-Cre mice and Graham Kay for the Tyr-Cre mice. Clones for riboprobe production were provided by: Fritz Meijlink (*Alx3*, *Alx 4* and *Cart1*); Jen Kuei Liu (*Dlx5*); Gail Martin (*Fgf8* and *Fgf10*); Vassillis Pachnis (*Lhx7*); Murray Hargrave (*Sox10*); John Rubenstein (*Dlx2*); Yi-Hsin Liu (*Msx2*); Eric Olson (*Twist2*); and Bill Shawlot (*Twist1*). Our work is supported by Mr. James Fairfax. HB is a University of Sydney and CMRI Postgraduate Scholar. DAFL is a Kimberly-Clark Research Fellow and PPLT is a Senior Principal Research Fellow of the NHMRC of Australia.

Appendix A. Supplementary data

Supplementary data associated with this article can be found, in the online version, at doi:10.1016/j.ydbio.2009.04.034.

References

Abe, M., Ruest, L.B., Clouthier, D.E., 2007. Fate of cranial neural crest cells during craniofacial development in endothelin-A receptor-deficient mice. Int. J. Dev. Biol. 51, 97–105.
Baker, C.V., Bronner-Fraser, M., Le Douarin, N.M., Teillet, M.A., 1997. Early- and late-migrating cranial neural crest cell populations have equivalent developmental potential in vivo. Development 124, 3077–3087.
Beverdam, A., Brouwer, A., Reijnen, M., Korving, J., Meijlink, F., 2001. Severe nasal clefting and abnormal embryonic apoptosis in Alx3/Alx4 double mutant mice. Development 128, 3975–3986.
Bialek, P., Kern, B., Yang, X., Schrock, M., Sosic, D., Hong, N., Wu, H., Yu, K., Ornitz, D.M., Olson, E.N., Justice, M.J., Karsenty, G., 2004. A twist code determines the onset of osteoblast differentiation. Dev. Cell 6, 423–435.
Castanon, I., Von, S.S., Kass, J., Baylies, M.K., 2001. Dimerization partners determine the activity of the Twist bHLH protein during *Drosophila* mesoderm development. Development 128, 3145–3159.
Chai, Y., Jiang, X., Ito, Y., Bringas Jr., P., Han, J., Rowitch, D.H., Soriano, P., McMahon, A.P., Sucov, H.M., 2000. Fate of the mammalian cranial neural crest during tooth and mandibular morphogenesis. Development 127, 1671–1679.
Chen, Y.T., Akinwunmi, P.O., Deng, J.M., Tam, O.H., Behringer, R.R., 2007. Generation of a Twist1 conditional null allele in the mouse. Genesis 45, 588–592.
Chen, Z.F., Behringer, R.R., 1995. twist is required in head mesenchyme for cranial neural tube morphogenesis. Genes. Dev. 9, 686–699.
Connerney, J., Andreeva, V., Leshem, Y., Mercado, M.A., Dowell, K., Yang, X., Lindner, V., Friesel, R.E., Spicer, D.B., 2008. Twist1 homodimers enhance FGF responsiveness of the cranial sutures and promote suture closure. Dev. Biol. 318, 323–334.
Connerney, J., Andreeva, V., Leshem, Y., Muentener, C., Mercado, M.A., Spicer, D.B., 2006. Twist1 dimer selection regulates cranial suture patterning and fusion. Dev. Dyn. 235, 1345–1357.
Danielian, P.S., Muccino, D., Rowitch, D.H., Michael, S.K., McMahon, A.P., 1998. Modification of gene activity in mouse embryos in utero by a tamoxifen-inducible form of Cre recombinase. Curr. Biol. 8, 1323–1326.
Depew, M.J., Tucker, A.S., Sharpe, P.T., 2002. Craniofacial Development. In: Rossant, J., Tam, PPL. (Eds.), Mouse Development. Academic Press, San Diego, pp. 421–498.
Evans, D.J., Noden, D.M., 2006. Spatial relations between avian craniofacial neural crest and paraxial mesoderm cells. Dev. Dyn. 235, 1310–1325.
Firulli, B.A., Krawchuk, D., Centonze, V.E., Vargesson, N., Virshup, D.M., Conway, S.J., Cserjesi, P., Laufer, E., Firulli, A.B., 2005. Altered Twist1 and Hand2 dimerization is associated with Saethre-Chotzen syndrome and limb abnormalities. Nat. Genet. 37, 373–381.
Fuchtbauer, E.M., 1995. Expression of M-twist during postimplantation development of the mouse. Dev. Dyn. 204, 316–322.
Gagan, J.R., Tholpady, S.S., Ogle, R.C., 2007. Cellular dynamics and tissue interactions of the dura mater during head development. Birth Defects Res., C Embryo Today 81, 297–304.
Gitelman, I., 1997. Twist protein in mouse embryogenesis. Dev. Biol. 189, 205–214.
Henrique, D., Adam, J., Myat, A., Chitnis, A., Lewis, J., Ish-Horowicz, D., 1995. Expression of a Delta homologue in prospective neurons in the chick. Nature 375, 787–790.

Hogan, B., Beddington, R., Costantini, F., lacy, E., 1994. Manipulating the mouse embryo: A laboratory manual, 2nd ed. Cold Spring Harbor Laboratory Press, Plainview, NY.
Ito, Y., Yeo, J.Y., Chytil, A., Han, J., Bringas Jr., P., Nakajima, A., Shuler, C.F., Moses, H.L., Chai, Y., 2003. Conditional inactivation of Tgfbr2 in cranial neural crest causes cleft palate and calvaria defects. Development 130, 5269–5280.
Jiang, X., Iseki, S., Maxson, R.E., Sucov, H.M., Morriss-Kay, G.M., 2002. Tissue origins and interactions in the mammalian skull vault. Dev. Biol. 241, 106–116.
Komori, T., Yagi, H., Nomura, S., Yamaguchi, A., Sasaki, K., Deguchi, K., Shimizu, Y., Bronson, R.T., Gao, Y.H., Inada, M., Sato, M., Okamoto, R., Kitamura, Y., Yoshiki, S., Kishimoto, T., 1997. Targeted disruption of Cbfa1 results in a complete lack of bone formation owing to maturational arrest of osteoblasts. Cell 89, 755–764.
Kuratani, S., Matsuo, I., Aizawa, S., 1997. Developmental patterning and evolution of the mammalian viscerocranium: genetic insights into comparative morphology. Dev. Dyn. 209, 139–155.
Laursen, K.B., Mielke, E., Iannaccone, P., Fuchtbauer, E.M., 2007. Mechanism of transcriptional activation by the proto-oncogene Twist1. J. Biol. Chem. 282, 34623–34633.
Lobe, C.G., Koop, K.E., Kreppner, W., Lomeli, H., Gertsenstein, M., Nagy, A., 1999. Z/AP, a double reporter for Cre-mediated recombination. Dev. Biol. 208, 281–292.
Loebel, D.A., Tsoi, B., Wong, N., O'Rourke, M.P., Tam, P.P., 2004. Restricted expression of ETn-related sequences during post-implantation mouse development. Gene. Expr. Patterns 4, 467–471.
MacKenzie, A., Ferguson, M.W., Sharpe, P.T., 1992. Expression patterns of the homeobox gene, Hox-8, in the mouse embryo suggest a role in specifying tooth initiation and shape. Development 115, 403–420.
McBratney-Owen, B., Iseki, S., Bamforth, S.D., Olsen, B.R., Morriss-Kay, G.M., 2008. Development and tissue origins of the mammalian cranial base. Dev. Biol. 322, 121–132.
Morriss-Kay, G.M., 2001. Derivation of the mammalian skull vault. J. Anat. 199, 143–151.
Noden, D.M., Trainor, P.A., 2005. Relations and interactions between cranial mesoderm and neural crest populations. J. Anat. 207, 575–601.
Ota, M.S., Loebel, D.A., O'Rourke, M.P., Wong, N., Tsoi, B., Tam, P.P., 2004. Twist is required for patterning the cranial nerves and maintaining the viability of mesodermal cells. Dev. Dyn. 230, 216–228.
Pietri, T., Eder, O., Blanche, M., Thiery, J.P., Dufour, S., 2003. The human tissue plasminogen activator-Cre mouse: a new tool for targeting specifically neural crest cells and their derivatives in vivo. Dev. Biol. 259, 176–187.
Rinon, A., Lazar, S., Marshall, H., Buchmann-Moller, S., Neufeld, A., Elhanany-Tamir, H., Taketo, M.M., Sommer, L., Krumlauf, R., Tzahor, E., 2007. Cranial neural crest cells regulate head muscle patterning and differentiation during vertebrate embryogenesis. Development 134, 3065–3075.
Soo, K., O'Rourke, M.P., Khoo, P.L., Steiner, K.A., Wong, N., Behringer, R.R., Tam, P.P., 2002. Twist function is required for the morphogenesis of the cephalic neural tube and the differentiation of the cranial neural crest cells in the mouse embryo. Dev. Biol. 247, 251–270.
Sosic, D., Richardson, J.A., Yu, K., Ornitz, D.M., Olson, E.N., 2003. Twist regulates cytokine gene expression through a negative feedback loop that represses NF-[kappa]B activity. Cell 112, 169–180.
Su, H., Mills, A.A., Wang, X., Bradley, A., 2002. A targeted X-linked CMV-Cre line. Genesis 32, 187–188.
Tonks, D., Nurcombe, V., Paterson, C., Zournazi, A., Prather, C., Mould, A.W., Kay, G.F., 2003. Tyrosinase-Cre mice for tissue-specific gene ablation in neural crest and neuroepithelial-derived tissues. Genesis 37, 131–138.
Vivatbutsiri, P., Ichinose, S., Hytonen, M., Sainio, K., Eto, K., Iseki, S., 2008. Impaired meningeal development in association with apical expansion of calvarial bone osteogenesis in the Foxc1 mutant. J. Anat. 212, 603–611.
Yoshida, T., Vivatbutsiri, P., Morriss-Kay, G., Saga, Y., Iseki, S., 2008. Cell lineage in mammalian craniofacial mesenchyme. Mech. Dev. 125, 797–808.